energies

MDPI

Article

Combined Bio-Hydrogen, Heat, and Power Production Based on Residual Biomass Gasification: Energy, Exergy, and Renewability Assessment of an Alternative Process Configuration

Mauro Prestipino *, Antonio Piccolo, Maria Francesca Polito and Antonio Galvagno

Department of Engineering, University of Messina, C.da di Dio 1, 98166 Messina, Italy; antonio.piccolo@unime.it (A.P.); polito.mariafrancesca@hotmail.it (M.F.P.); antonio.galvagno@unime.it (A.G.)
* Correspondence: mauro.prestipino@unime.it

Abstract: Bio-hydrogen from residual biomass may involve energy-intensive pre-treatments for drying and size management, as in the case of wet agro-industrial residues. This work assesses the performance of an alternative process layout for bio-hydrogen production from citrus peel gasification, with the aim of cogenerating heat and power along with hydrogen, using minimal external energy sources. The process consists of an air-steam fluidized bed reactor, a hydrogen separation unit, a hydrogen compression unit, and a combined heat and power unit fed by the off-gas of the separation unit. Process simulations were carried out to perform sensitivity analyses to understand the variation in bio-hydrogen production's thermodynamic and environmental performance when the steam to biomass ratios (S/B) vary from 0 to 1.25 at 850 °C. In addition, energy and exergy efficiencies and the integrated renewability (IR) of bio-hydrogen production are evaluated. As main results, the analysis showed that the highest hydrogen yield is 40.1 kg_{H2} per mass of dry biomass at S/B = 1.25. Under these conditions, the exergy efficiency of the polygeneration system is 33%, the IR is 0.99, and the carbon footprint is −1.9 $kg_{CO2\text{-}eq}/kg_{H2}$. Negative carbon emissions and high values of the IR are observed due to the substitution of non-renewable resources operated by the cogenerated streams. The proposed system demonstrated for the first time the potential of bio-hydrogen production from citrus peel and the effects of steam flow variation on thermodynamic performance. Furthermore, the authors demonstrated how bio-hydrogen could be produced with minimal external energy input while cogenerating net heat and power by exploiting the off-gas in a cogeneration unit.

Keywords: bio-hydrogen; wet biomass; gasification; CHP; bioenergy; citrus peel; polygeneration; integrated renewability; exergy efficiency; carbon-neutral hydrogen

Citation: Prestipino, M.; Piccolo, A.; Polito, M.F.; Galvagno, A. Combined Bio-Hydrogen, Heat, and Power Production Based on Residual Biomass Gasification: Energy, Exergy, and Renewability Assessment of an Alternative Process Configuration. *Energies* **2022**, *15*, 5524. https://doi.org/10.3390/en15155524

Academic Editor: Jaroslaw Krzywanski

Received: 27 June 2022
Accepted: 27 July 2022
Published: 29 July 2022

1. Introduction

In recent years, hydrogen has gained additional importance in transitioning to "net-zero by 2050" in the energy sector on a global scale [1]. Hydrogen and hydrogen-based fuels will increase from 1% of today's total final energy consumption to 13% in 2050 globally [2]. Hydrogen must be produced from renewable and sustainable resources (solar, wind, hydro, or biomass energy) to comply with a net-zero future. Sustainable biomass is a renewable primary energy resource that can be converted into renewable liquids, gas (including hydrogen), and electricity using biochemical or thermochemical approaches. Thermochemical gasification is an efficient and effective approach for the conversion of biomass to hydrogen (also defined as bio-hydrogen since it is produced from biomass). A further advantage of using biomass as feedstock is the possibility of producing carbon-neutral or carbon-negative fuels, heat, cold, or power [3], depending on the specific process configuration and the impact on the whole production chain.

"Almost-carbon-neutral" hydrogen production can be achieved if fossil fuels are needed along the entire production chain (feedstock transportation, feedstock pre-treatment, etc.).

Residual biomasses are attractive feedstocks to be deployed for thermochemical conversion because they do not require additional land dedicated to biomass cultivation and can generate additional revenue for farmers and food industries (e.g., factories that convert vegetables and fruits into final food products). It follows that the sustainable use of residual biomass can help decarbonize the agricultural and food conversion sectors. However, thermochemical processes such as gasification need dry feedstock as input into the reactors, which has moisture content usually in the range of 10–20% in mass [4], while residual biomasses from the food and drink industry are generated with a high moisture content. This is the case of residue from the juice factories, which convert fruits into juice, generating large amounts of solid residue with a water content of 50–70%. However, energy-intensive thermal pre-treatments are needed to use wet biomass as gasification feedstock. For example, citrus peel is a wet residue with a water content of 60–70% after mechanical pressing, which is usually dried (when needed) using Natural Gas (NG). Galvagno et al. [5] analyzed citrus peel gasification coupled with a cogeneration unit (for combined heat and power—CHP) and a citrus juice factory. Via process simulation, they demonstrated that proper thermal integration and plant size could reduce the carbon impacts of the citrus juice industry. In addition, the Life Cycle Assessment (LCA) of citrus peel-based gasification-CHP demonstrated the thermodynamic and environmental advantages of this integration with the juice industry compared to the reference scenarios [6].

Among the different gasification technologies, fixed bed gasifiers can be deployed with a simple design and construction [7]. However, these technologies are limited in scale [8]; they are affected by high residence time [9], and specific particle size and shape of feedstocks are required [10]. Contrarily, fluidized bed gasifiers can be easily scaled-up; they allow a short residence time with high carbon conversion, and they can be fed with a variety of feedstocks [11].

Entrained flow gasifiers may achieve high carbon conversion at a very short residence time [12] due to the high temperature. For the same reason, syngas with low tar concentration is produced [13].

Indirect gasification for hydrogen production is an alternative option to generate high-quality syngas streams, due to the absence of nitrogen and combustion products [14]. This technology has been also improved by Pallozzi et al. [15] by including catalytic candles to further upgrade the syngas quality within the reactor.

Yao et al. [16] conducted a techno-economic analysis of different pathways for renewable hydrogen production, including biomass gasification, biogas reforming, and water electrolysis. Their results showed that gasification could generate more cost-efficient renewable hydrogen than alkaline electrolysis. In addition, they showed that, in the case of bio-hydrogen from gasification, freshwater consumption is three times lower than electrolysis. As in the research paper of Yao et al., the most common process layout for bio-hydrogen production consists of air or air–steam gasification coupled with water–gas shift (WGS) conversion to increase the hydrogen yield, leading to about 0.057 kg_{H2}/kg_{biom} on a dry basis [16]. On the other hand, sorption-enhanced gasification is an interesting alternative process configuration for hydrogen production [17] via biomass gasification. It avoids using WGS, reduces water consumption and syngas cleaning steps, and generates about 0.046 kg_{H2}/kg_{biom} [17].

The process layouts and concepts for bio-hydrogen production described above need external power to cover the consumption of the process' auxiliaries because the syngas is converted mainly into CO_2 and H_2. In addition, a relevant amount of heat is needed when dealing with wet residues.

In this work, the authors present an alternative process configuration for bio-hydrogen production through gasification of citrus peels as waste of an agro-industrial factory. The main units of the proposed design are: (i) an air–steam fluidized bed gasifier, (ii) a Pressure Swing

Adsorption (PSA) unit for hydrogen separation, (iii) an internal combustion engine for combined heat and power (CHP), (iv) and a hydrogen compression unit with heat recovery. The off-gas of the PSA unit feeds the CHP unit after hydrogen separation. This stream consists of carbon monoxide, methane, carbon dioxide, nitrogen, and residual hydrogen. The proposed system does not use WGS units or complex dual fluidized bed reactors with sorption loops, which would lead to a slight reduction in hydrogen yield.

The impacts of process parameters on the system's yields, efficiencies, and renewability degree are assessed by sensitivity analysis. The thermodynamic performance is based on exergy data, while the renewability degree of bio-hydrogen is evaluated by the "Integrated Renewability" indicator, recently introduced by Prestipino et al. [6]. The proposed configuration's advantage relies on the possibility of cogenerating, along with hydrogen, electricity, and heat that can be exploited to cover the process heat and power demand. Furthermore, residual net heat and power can be delivered to external users. The aim is to make the process independent of external energy input, even in the case of wet residues, and to simplify the process configuration. The selected process layout covers the energy-intensive drying step when wet residual biomass is involved, in addition to the internal consumption.

Furthermore, this is the first paper exploring the potential of citrus peel gasification for bio-hydrogen production. Despite the specificity of the feedstock, the analysis can be extended to the exploitation of a variety of wet feedstocks.

The outcomes of this work are fundamentals to investigate alternative polygeneration systems using wet residues that are currently unexploited for bio-hydrogen production. The implementation of such systems at the local and regional scale can mitigate the impacts on the food processing industry. To do so, proper process integrations must be investigated.

From the above, this paper intends to cover the lack of research works regarding sensitivity analysis and renewability of processes where bio-hydrogen, net heat, and power production is accomplished simultaneously by exploiting the off-gas from the hydrogen separation unit.

2. Materials and Methods

2.1. Process Description

Figure 1 shows the proposed polygeneration system for Combined Hydrogen, Heat, and Power (CHHP) production fed by citrus peel. For simplification, the schematic represents just the main units and streams. The system consists of a thermal dryer that reduces the humidity of citrus peel from about 65% to 15%(*w*/*w*), a gasification unit, a two-stage syngas compression section coupled with a Pressure Swing Adsorption (PSA) unit for hydrogen separation, pure hydrogen compression, and an internal combustion engine. The off-gas (#20 Off-gas) of the PSA (containing mainly CO, CO_2, N_2, and CH_4) feeds the internal combustion engine, which is configurated in cogeneration mode for Combined Heat and Power production (CHP). The thermal integration between the different sections of the system and the integration with the factory is provided by heat exchangers (HE) to recover sensible enthalpy from hot streams.

The drying section is driven by heat recovered in the CHP unit (#41) and the hydrogen (#40) and syngas compression sections (#34). The heat carrier, in this case, is hot water at 120 °C and 2.5 bar. After the drying step, the dry biomass (#2) is sent to the Bubbling Fluidized Bed (BFB) reactor operated at 850 °C. The Steam to Biomass (S/B) ratio is varied in the range of 0–1.25 to assess the effects of its variation on hydrogen yield and thermodynamic performance. The syngas (#3) passes through a cyclone, then it is cooled from 750 to 200 °C. The heat recovery from syngas colling is used to convert hot water to superheated steam (2 bar; 250 °C) in HE1, used as a gasification agent. After this stage, the syngas is at a temperature varying between 300 and 600 °C, depending on the S/B. The higher the steam flow rate, the lower the syngas temperature after providing heat to the gasification agents. Then, gasification air is heated up to 250 °C before entering the reactor, reducing the syngas temperature further. The residual syngas enthalpy is recovered by cooling it to 200 °C and

heating water from 80 °C (#31) to superheated water at 120 °C (in HE3). The S/B influences the mass flow rate of this stream. The syngas temperature is kept higher than 200 °C to reduce the risk of massive tar condensation before entering the scrubber. Here, tars are removed, and the syngas is cooled to about 40–50 °C in the scrubbing process [18].

The syngas is then delivered to the compression unit, where it is compressed to 7 bar in a two-stage compressor with heat recovery (HE4). Here, hot water is heated from 80 to 120 °C in HE4. The compressed syngas (#10) is then directed to the PSA unit where hydrogen (99.9% purity) is separated from other permanent gases. The hydrogen separation efficiency in the PSA unit is 70%(wt/wt) [15]; hence, 30% of hydrogen in the syngas is available in the off-gas (#20).

The off-gas is used in the CHP unit, which has electrical and thermal efficiencies of 37.1% and 44.3%, respectively. In this work, the authors selected a CHP unit produced by INNIO-Jenbacher, model JMS 316 GS-S.L (611 kWe output). In case the off-gas' LHV is lower than 5.4 MJ/Nm^3, which is the LHV value prescribed by the manufacturer, natural gas (NG) is mixed with the off-gas streams entering the CHP unit. The NG's flow rate is calculated to reach the target LHV. In the cogeneration unit, the heat is recovered as superheated water at 120 °C, and it is directed to a collector where it is mixed with superheated water from HE3 and HE4 (heat recovery from syngas cooling). The sum of these streams (43) can be used in the drying unit and the juice factory. In this work, the cogenerated and recovered heat is directed primarily to the drying section to design an energy-self-sufficient bio-hydrogen polygeneration system. If the heat demand of the dryer is covered, the residual heat can be directed to the factory (stream 44). A fraction of power generated in the CHP unit is used for driving the compressors shown in Figure 1 and all the auxiliaries that are not included in the schematic, such as pumps, biomass feeders, fans, actuators, controllers, etc. The power consumption due to these ancillaries is allocated as 15% of the generated power [19] if all syngas would be delivered to the CHP unit (without hydrogen separation). The power demand for syngas and hydrogen compression is determined separately in this work, while the isentropic efficiency of syngas and hydrogen compressors is 72%.

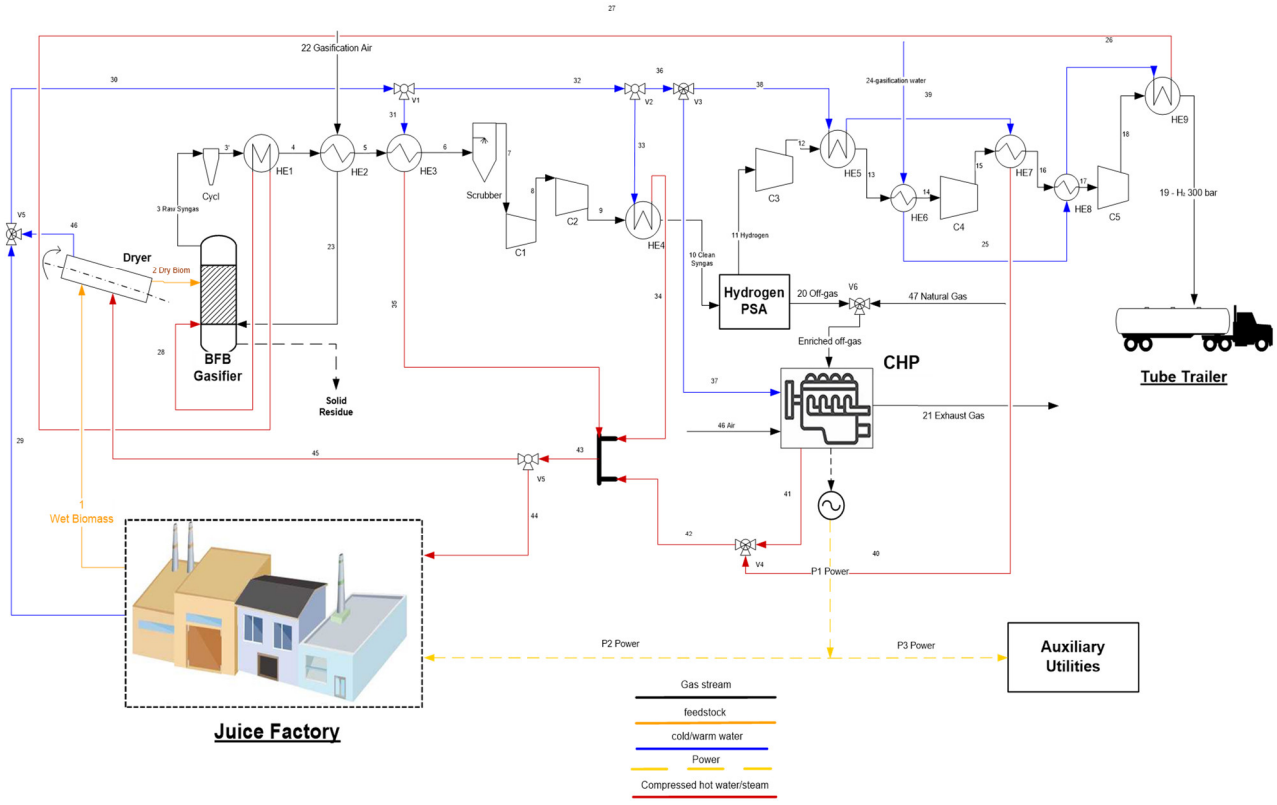

Figure 1. Layout of the polygeneration system.

The pure hydrogen stream (#11) is compressed from atmospheric pressure to 300 bar in a three-stage compression unit with intercooling for heat recovery. Hydrogen is first cooled by heating the return water from the dryer and the factory (38) from 80 to 120 °C (HE5 and HE7). In the first and second compression stages, the described hydrogen cooling is followed by a second cooling (HE6 and HE8) where a variable cold-water flow (stream 24, 0–1.25 kg/h per kg/h of biomass) is pre-heated before being converted into steam, used as gasification agent. After compressor C5 (the third and last hydrogen compression stage), the hydrogen is cooled in one step by exchanging with the gasification water pre-heated in the first and second compression stages (stream 26). This last cooling stream is heated up to 75–120 °C, depending on the S/B value. Then, it passes through the first heat exchangers for syngas cooling (HE1), where it is converted into superheated steam at 250 °C and 2 bar. If the internal heat demand (i.e., drying and gasification agents) cannot be covered by cogenerated or recovered heat, hydrogen spillage can be applied.

The list of the streams represented in Figure 1 with the flow rates, physical properties, and mass composition is included in the AppendixA section.

2.2. Performance Indicators

The thermodynamic and environmental performances of the proposed system are evaluated in terms of energy yield, energy and exergy efficiencies, and renewability degree of bio-hydrogen. The energy yields (Y_{Ei}) (MJ/kg) and the hydrogen mass yield (Y_{mH2}) (kg/kg) per unit of biomass input are calculated according to the following equations:

$$Y_{Ei} = \frac{E_i}{m_{biom\_db}} \quad (1)$$

$$Y_{mH2} = \frac{m_{H2}}{m_{biom\_db}} \quad (2)$$

where E_i (MJ) and m_{biom_db} (MJ) stand for the energy output (hydrogen, electricity, and heat) and the mass of biomass fed into the reactor on a dry basis, respectively, while m_{H2} indicates the mass of hydrogen produced.

The energy and exergy efficiencies of bio-hydrogen and the whole system are assessed as follows:

$$\eta_{H2} = \frac{E_{H2}}{E_{biom} + E_{el} + E_{NG}} \quad (3)$$

Here, E_{H2} indicates the hydrogen energy (LHV), which is considered in this indicator as the only output energy stream since the hydrogen energy efficiency is evaluated. The energy input is indicated by E_{biom}, which is the energy input provided by biomass (LHV basis), E_{el} is the external electricity input needed to power the auxiliaries, and E_{NG} is the sum of natural gas input (LHV Basis) used to increase the LHV of the off-gas feeding the ICE engine.

The following equation describes the exergy efficiency of bio-hydrogen produced with the proposed system, where the subscription *ex* refers to the exergy of the same terms described above.

$$\eta_{ex\_H2} = \frac{E_{ex\_H2}}{E_{ex\_biom} + E_{ex\_el} + E_{ex\_NG}} \quad (4)$$

The energy and exergy efficiencies of the whole polygeneration system are reported in Equations (5) and (6), respectively. Here, E_{elCHP} is the electrical energy generated by the cogeneration unit, E_{th} is the sum of thermal energy recovered in the cogeneration unit and the other sections (syngas and hydrogen cooling) of the process described above.

$$\eta_{system} = \frac{E_{elCHP} + E_{th} + E_{H2}}{E_{biom} + E_{el} + E_{CH4}} \quad (5)$$

$$\eta_{ex\_system} = \frac{E_{ex\_elCHP} + E_{ex\_th} + E_{ex\_H2}}{E_{ex\_biom} + E_{ex\_el} + E_{ex\_NG}} \quad (6)$$

The renewability degree of bio-hydrogen produced according to the proposed polygeneration system is assessed considering the exergy of non-renewable energy streams. For the NG stream, the chemical exergy was considered. In addition, the net cogenerated streams (electricity and heat after subtracting the internal heat and power consumption) are delivered to the juice factory and considered as substitutes for the existing energy sources. Specifically, net cogenerated heat is intended to substitute natural gas for heat production, while net cogenerated power replaces electricity from the grid. Despite many juice factories already using NG dryers to dry the citrus residues before selling or disposal, heat for drying is considered an internal consumption of the proposed bio-hydrogen production system, in this work.

In Equation (7), the exergy of biomass is calculated according to the approximate expression defined in [20].

$$E_{ex\_biom} = 1.047\ HHV_{biom} \quad (7)$$

The exergy of mass streams, as for hydrogen at 300 bar, is calculated as the sum of the physical (E_{ex_ph}) and chemical ($E_{ex_{ch}}$) exergies (MJ) that are described in Equations (8)–(10).

$$E_{ex\_ph} = m(h - h_0 - T_0(s - s_0)) \quad (8)$$

In the previous equation, h and s stand for the specific enthalpy and entropy, respectively, while m stands for the mass of the species considered. The subscript 0 describes the reference state of temperature and pressure, which is 293 K and 1 bar, in this work. In the exergy equations, the unit of measurement of temperature is K, while for pressure it is Pa.

In the case of perfect gas, E_{ex_ph} can be calculated as:

$$E_{ex\_ph} = mc_{pm}\left(T - T_0 - T_0 ln\frac{T}{T_0}\right) + RT_0 ln\frac{P}{P_0} \quad (9)$$

The chemical exergy reported in Equation (10) is defined by the specific chemical exergy of the i-th component (ex_i^{ch}) and its mass fraction x_i in the considered stream.

$$E_{ex\_ch} = m(\sum x_i ex_i^{ch} + RT_0 \sum x_i \ln x_i) \quad (10)$$

The exergy associated with heat recovery is calculated according to Equation (11), where Q is the heat exchanged, while T_0 and T_j are the temperature of the reference state and the temperature of the hot stream input, respectively.

$$E_{exQ} = \left(1 - \frac{T_0}{T_j}\right) Q \quad (11)$$

In a previous research work [6], the authors already defined the Integrated Renewability (*IR*) of an energy product as its renewability degree when the energy production system is integrated with a specific industrial environment that can be supplied with the cogenerated secondary streams (e.g., as in the case of biohydrogen production integrated with the citrus juice factory). The IR applied in this work is described in Equation (12).

$$IR = \frac{E_{P\_ex} - netEx_{nr}}{E_{P\_ex}} \quad (12)$$

$$netEx_{nr} = grossEx_{nr} - Ex_{AVnr} \quad (13)$$

where $grossEx_{nr}$ is the exergy of the non-renewable resources used for bioenergy production, while Ex_{AVnr} is the exergy of non-renewable resources that are avoided using cogenerated energy streams (heat and power). As it is designed, the IR can reach values >1 when more non-renewable exergy is avoided than it is used to generate the unit of the renewable exergy product (E_{P_ex}). When 0 < *IR*< 1, the exergy product is not fully renewable and has a certain degree of renewability.

In this work, the environmental and thermodynamic performances are evaluated considering the direct impacts of the presented bio-hydrogen production process since the detailed Life Cycle Analysis (LCA) is not the object of the present work. When the non-renewable exergy of electricity must be determined, the authors limited the analysis to the direct use of non-renewable fuels in the national mix to produce the unit of electricity. According to the Italian Superior Institute for the Environmental Research and Protection (ISPRA) [21], the non-renewable electricity production in Italy was 60.5% of the total national production in 2019.

The following equation has been used to calculate the non-biogenic *GHG* emissions.

$$GHG = \frac{E_{NG} f_{NG} - E_{CHP\_el} f_{el} - \frac{E_{CHP\_h} f_{NG}}{\eta_{boiler}}}{m_{H2}} \left[\frac{\mathrm{kgCO_{2-eq}}}{\mathrm{kg_{H2}}}\right] \quad (14)$$

where E_{NG}, E_{CHPel}, and E_{CHP_h} stand for the energy of natural gas (LHV-based) used in the internal combustion engine with the off-gas, the cogenerated electricity, and the cogenerated heat, respectively. The emission factors of natural gas and electricity from the national grid are indicated by f_{NG} and f_{el}, respectively. The thermal efficiency of the natural gas boiler was assumed to be 0.9.

The ISPRA database was used to obtain the emission factors of electricity production and natural gas combustion in Italy, which are 0.0750 kg $CO_{2\text{-}eq}$/MJ_e and 0.0579 kg $CO_{2\text{-}eq}$/MJ_{CH4}, respectively [21]. The methodology used for the calculations of the emission factors follows the IPCC 2006 guidelines [21].

2.3. Gasification Model

The simulation model of the gasifier is developed in the AVEVA PROII Simulation 2021 environment using a thermodynamic equilibrium model that uses a non-stoichiometric approach. This method is based on the minimization of the total Gibbs free energy of the reacting system. At a specific temperature and pressure, the total Gibbs free energy (G^T) of a multi-phase system with multi-components was defined by Equation (15):

$$\frac{G^T}{RT} = \sum_{j=1}^{NS} \frac{G^{\circ C}_j}{RT} n^C_j + \sum_{p=1}^{NP} \sum_{f=1}^{NF} \frac{G_{fp}}{RT} n_{fp} \quad (15)$$

where *NS* is the number of solid components, *NP* is the fluid-phase number, and *NF* is the number of components at fluid phase; $G^{\circ C}_j$ stands for standard free Gibbs energy of each solid component, while G_{fp} is the free Gibbs energy of fluid components at a given pressure and temperature; and n^C_j ed n_{fp} are moles of each species in solid products and in fluid-phase products.

The minimization of Gibbs free energy can be resolved by placing the derivative of $\frac{G^T}{RT}$ equal to zero. By solving the equations system, the number of moles of each component can be determined. To solve the system, the constraints of mass balance on the chemical elements that are part of the system can be utilized since they require mass conservation. Then, the Lagrange Multiplier method was applied [22]. The Soave–Redlich–Kwong (SRK) equation of state has been chosen to describe each component's behavior and its relative thermodynamic properties. SRK model is recommended for systems operating at

moderate to high temperatures involving hydrocarbons and other permanent gases (e.g., hydrogen, carbon dioxide, carbon monoxide, and nitrogen) [23].

The thermodynamic equilibrium method is helpful in modeling processes without information about the reactor geometry or the reactions involved. However, it has limitations: it is not possible to compute Tar, the heat losses associated with the process, and the influence of fluid dynamic properties of the reagents used and reactor configuration. Model simplifications can also lead to overestimating the amount of hydrogen obtained. Finally, the method may not be applicable if gasification is at relatively low temperatures.

Nevertheless, equilibrium modeling remains the most used, as it provides the basic parameters of the process and its theoretical limits.

Since tar generation is not thermodynamically favored, it cannot be computed in the model, and it is neglected in this work. Similarly, the model is limited in computing methane formation. However, since methane is formed experimentally in percentage, its energy content cannot be neglected.

For this reason, a relation for the CH_4 flowrate as a function of the Steam-to-Biomass Ratio (S/B) was introduced in the model, which is obtained from the experimental data of Galvagno et al. [5]:

$$\mathrm{CH_4}\left[\frac{\mathrm{kg}}{\mathrm{s}}\right] = (0.0576 - 0.0102\,S/B)B$$

where S (kg/s) and B (kg/s) stand for the steam and biomass flow rates, respectively.

Simulation has been created by using the Organic Industrial Wastes ultimate analysis on a dry basis, which is shown in Table 1.

Table 1. Elemental composition of the feedstock (citrus peel) on a dry basis.

Element	C	H	O	N	S	Ash
Concentration (% m/m$_{db}$)	43	6.3	42.3	1.3	0.1	7

In this work, the simulation of gas cleaning steps for tar, sulfur, and nitrogen compounds is not considered since it is not the object of this analysis. Furthermore, well-established and commercial syngas cleaning processes, with negligible impacts on the energy balance of the system, are available in the literature. A virtual heat exchanger is included to simulate the temperature reduction in syngas when it is subjected to the scrubbing process.

2.3.1. Gasification Unit

The model of the gasification unit consists of two decomposition blocks. At first, biomass is introduced in the reactor block named *Solid Fuel Combustor* (*Decomp*), where its decomposition into the primary chemical species is simulated according to the following reaction obtained from the mass balance. Then, the software calculates the molar weight of biomass from the ultimate analysis introduced as input data.

$$Biomass \rightarrow 897.6\,C + 789\,H_2 + 11.6N_2 + 0.782S + 331.11O_2 + 29.22ASH$$

In this reactor, no temperature increase has been computed.

The reaction provides *H*, *N*, *O*, and *S* in the gas phase and char and ashes as solid residues. Char is modeled as solid carbon, while ashes are modeled as SiO_2. Both phases are fed to a second block: the solid fuel combustor (*Gass*) simulating char and volatile components gasification using air and steam as gasification agents, which are introduced into the reactor at 523 K and 200 kPa.

The gasification reactor is set to work at 1123 K with a temperature approach of 50K. Here, based on previous works [5], a carbon conversion of 97% has been assumed for the following solid–gas reactions.

$$C + O_2 \rightarrow CO_2$$

$$C + CO_2 \leftrightarrow 2CO$$

$$C + H_2O \leftrightarrow CO + H_2$$

The same block allows the minimization of the Gibbs free energy of formation and the definition of syngas composition.

The gasification unit model is shown in Figure 2.

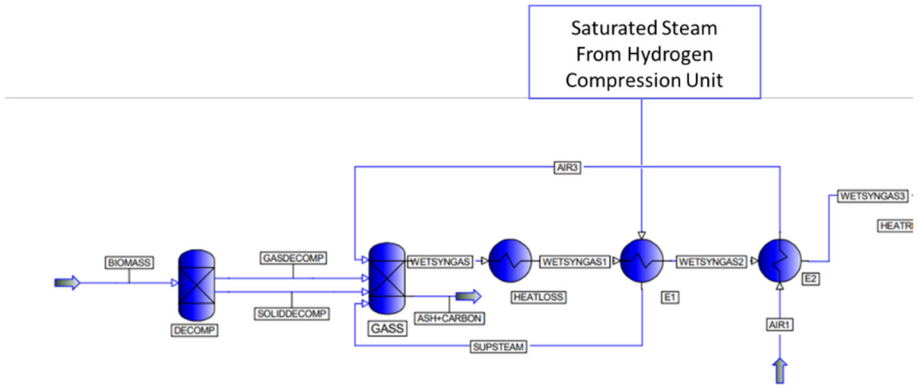

Figure 2. Simulation model of the gasification unit in *AVEVA PRO II Simulation*.

Wet and hot syngas (*#WETSYNGAS* in Figure 2) exits the reactor at 1023 K (a simple heat exchanger simulates the temperature reduction), and it is then directed to heat exchangers that are used to transfer the syngas' sensible enthalpy to saturated steam (*E*1) and air (*E*2) used as gasification agents.

The first step of sensible heat recovery from syngas is obtained in a superheater to heat the saturated steam to 523 K. Then, the still-hot syngas (*#WETSYNGAS2*) heats the air to 523 K.

As reported in Figure 3, the remaining residual heat (*#WETSYNGAS3*) is used to produce hot water at 393 K and 2.1 bar (*#W2*), which is then cooled to 353 K by another user (e.g., for feedstock drying or in the citrus juice factory). To prevent massive tar condensations, the latter HE (*HEATRECOVER1*) is set to cool the syngas to 473 K. Since tar formation is neglected in this work, the temperature reduction in syngas that occurs in the scrubbing unit is simulated by an additional heat exchanger (*SCRUBBING*). Water condensation is simulated by a flash separator (*FLASHCOOLER1*).

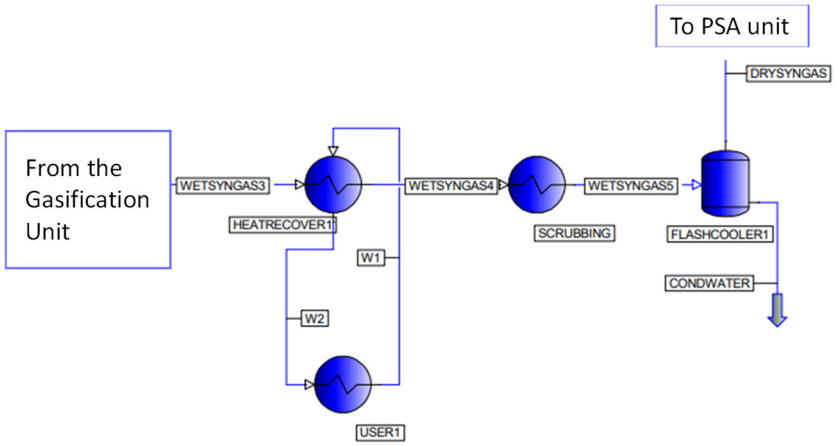

Figure 3. Simulation model of syngas cooling, cleaning, and drying in AVEVA PRO II Simulation.

2.3.2. PSA Unit

Dry syngas is fed to a Pressure Swing Adsorption Unit (PSA), which aims to separate hydrogen from other gaseous components by exploiting gas adsorption properties as pressure changes. The simulation model of this unit is reported in Figure 4.

This unit is modeled as a two-stage inter-refrigerated compression followed by a separation unit at room temperature. The cooling step after the second compression stage (C2), is performed by two heat exchangers: the first exchange (*#HEATRECOVER2*), simulating a thermal recovery, is operated by water at 343 K and 200 kPa, reaching 393 K at the end of the heating. As in the previous section, the user of the recovered heat is simulated by a simple heat exchanger that reduces the temperature of the hot stream to 353 K. In compressors' modeling, a mechanical efficiency of 0.9 and an adiabatic efficiency of 0.72 has been assumed. The hydrogen from the PSA is directed to the following hydrogen compression unit, while the off-gas is directed to the CHP unit described above. The block used for simulating the actual hydrogen separation is a *Stream Calculator* block, where a hydrogen recovery rate is set to 70% (separation efficiency reported by Pallozzi et al. [15]).

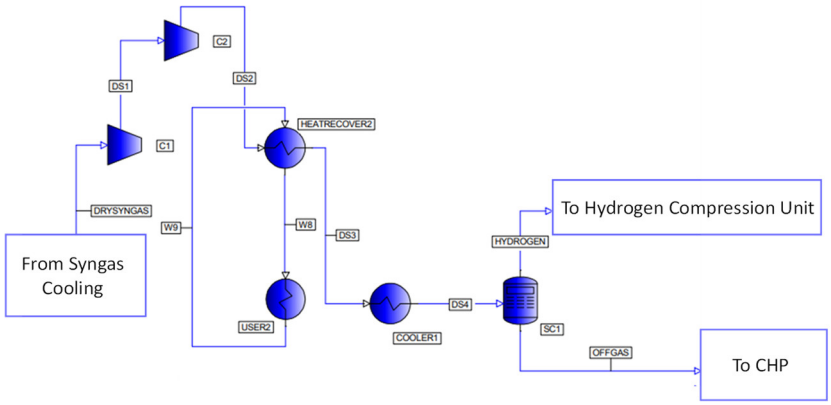

Figure 4. Simulation model of the PSA section in AVEVA PRO II Simulation.

2.3.3. Hydrogen Compression Unit

Hydrogen from the PSA is fed to a compression unit (Figure 5), where it is compressed to 300 bar. This operation is carried out through three inter-refrigerated compression stages, where cooling is performed by HEs recovering heat used for pre-heating the gasification agents. Each intercooling stage consists of a HE that simulates the high-temperature heat recovery and a heat exchanger that simulates low-temperature heat recovery. After the first compression, the hydrogen stream is cooled by the return water from the user at 353 K (*#w3*), leading to saturated steam at 393 K (*#w4*) after the second compression step. The second HE of each compression stage is fed by water at 293 K (*#water*) that progressively generates saturated steam used as a gasification agent. This stream is then directed to the gasification unit to be converted into superheated steam by exchanging heat with hot syngas.

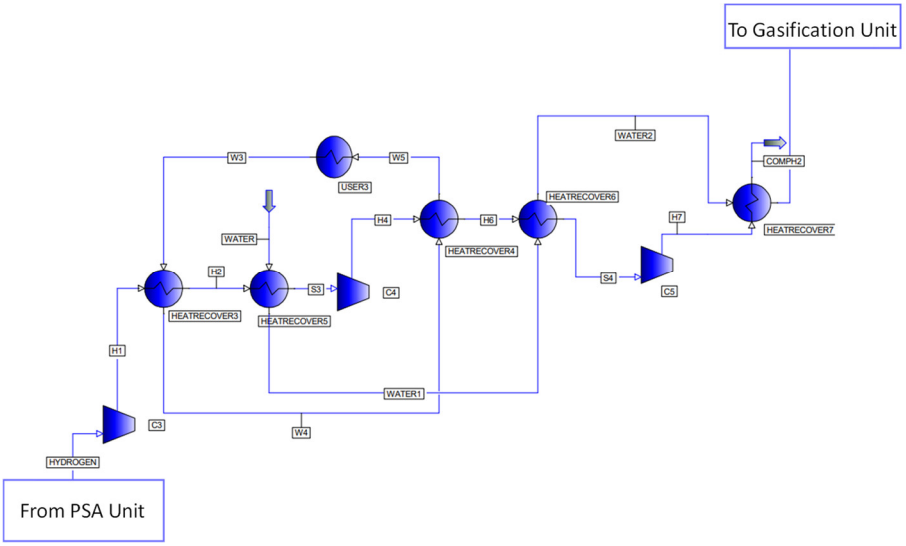

Figure 5. Simulation of the hydrogen compression unit in AVEVA PRO II Simulation.

2.4. Model Validation

Simulated data have been related to experimental data obtained in a previous work [24] using a laboratory-scale BFB plant as the S/B ratio varied in the range 0–1.25 at 850 °C. Results of validation shown in Figure 6 reveal that increasing the S/B ratio leads to a higher hydrogen and carbon dioxide percentage due to the reduction in carbon monoxide content. As a result of the increased number of reagents that are fed into the process, the nitrogen concentration decreases due to the progressive increase in the mass flow rates of hydrogen, carbon dioxide, and carbon monoxide. This indicates that the syngas yield increases together with the S/B ratio. Methane is not reported in the validation graph because the correlation of its productivity with the S/B ratio has been introduced as an input. Figure 6 shows that the model fits the experimental data.

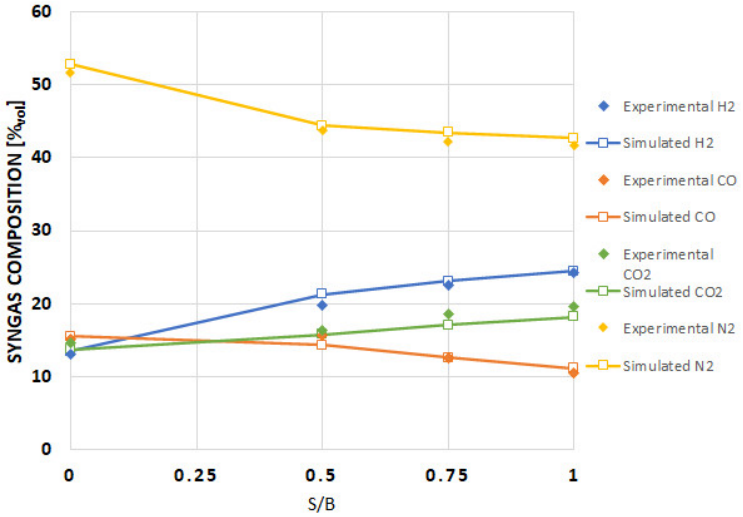

Figure 6. Model validation by syngas composition (%vol/vol).

3. Results and Discussion

The energy yields of the cogenerated energy streams of the proposed polygeneration system are reported in Figure 7 at different S/B. In the same figure, the hydrogen mass yield is shown as well (blue line). As expected, the hydrogen yield increases as the steam to biomass ratio increases. Both mass and energy yields are expressed per ton of dry

biomass. Specifically, the hydrogen energy yield increases from 1992 MJ/t_{db} to 4805 MJ/t_b. Therefore, in terms of mass, the hydrogen yield ranges from 16.6 to 40.1 kg_{H2}/t_{db}.

As expected, the highest hydrogen yields reached in this work are lower if compared with other process configurations involving intensive water–gas shift (WGS) steps or the innovative sorption enhanced gasification [17]. Specifically, the new WGS process integrated with a dual fluidized bed proposed by Yao et al. generates about 57 kg of hydrogen per ton of biomass (on a dry basis) [16]. Regarding the sorption enhanced gasification technology (SEG), the IEA bioenergy report [17] shows that about 46 kg_{H2}/t_{db} can be produced without using a WGS unit, which is 15% higher than the simplified hydrogen and polygeneration production process proposed in this work. Compared to the process presented in this work, SEG-based hydrogen production consumes 10% more fresh water per kg of H_2.

Net electricity production shows the maximum yield at S/B = 0 (1928 MJ/t_{db}). When steam is introduced, the electricity yield slightly decreases to 1779 MJ/t_{db} at S/B = 0.125 and then is kept stable in the range 1780–1800 MJ/t_{db} when the S/B increases. The reduction in electricity yield when switching from air and air–steam gasification is mainly due to the rise in internal electricity consumption for water pumping and hydrogen compression. In the case of air–steam gasification within the investigated S/B values, the almost constant electricity yield is due to the increased addition of natural gas to the off-gas stream that feeds the CHP unit. As described in the methods section, natural gas is needed to keep the off-gas LHV at values recommended by the engine manufacturer (5.4 MJ/Nm^3).

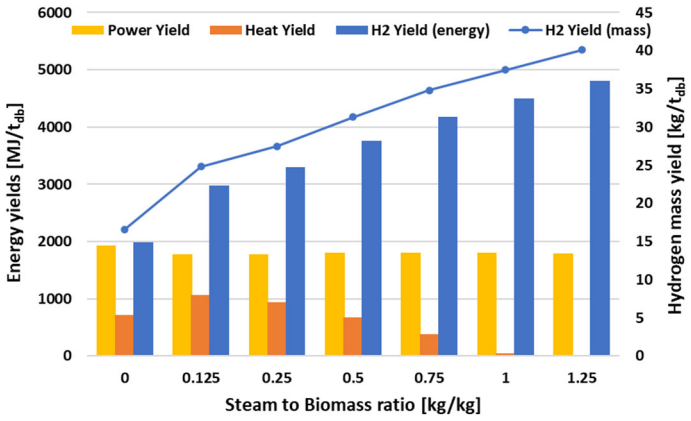

Figure 7. Energy and mass yields as a function of the steam to biomass ratio.

Heat production is increased when S/B is switched from 0 to 0.125. In this case, the increased internal consumption due to steam production is more than compensated by augmented energy production in the CHP unit due to higher syngas and off-gas yield when steam is added as a gasification medium. However, further steam addition reduces the available heat due to the progressive rise in internal consumption. Therefore, at S/B = 1.25, no heat is available for recovery. Indeed, at S/B = 1.25, a small amount of external heat is needed to air pre-heating (251 MJ/t_{db}) and feedstock drying (78 MJ/ton_{db}), which is obtained by spilling hydrogen before compression to 300 bar. As an alternative solution, NG can be used as backup fuel to cover the residual heat demands at high S/B conditions.

Figure 8 shows the hydrogen energy and exergy efficiencies as a function of the S/B. The difference between the black and red dots at S/B = 1.25 lies in the feedstock used to cover the residual heat demand described above. The red pointers refer to the case of hydrogen spilling (reduction in energy/exergy output), while the black ones refer to the case of additional use of NG (increased energy/exergy input). The introduction of steam to the gasification process clearly improves energy and exergy hydrogen efficiencies, reaching 0.26 and 0.24, respectively, at S/B = 1.25. The almost linear increase in the hydrogen efficiencies from S/B = 0.12 to 1.25 is consistent with the hydrogen yield trend.

A slight reduction in the hydrogen efficiencies (about 5%) is observed when bio-hydrogen is spilled to cover the residual heat demand of the process (S/B = 1.25).

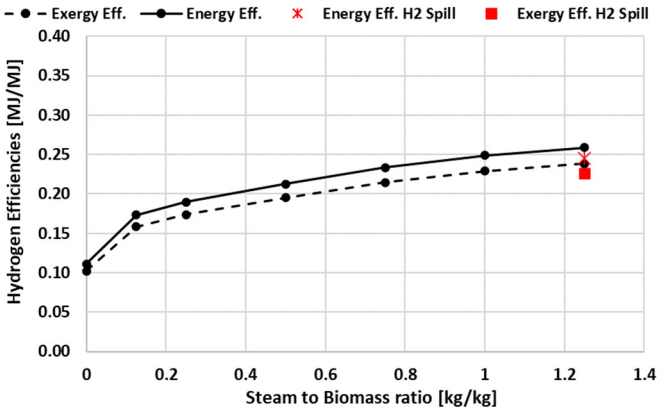

Figure 8. Hydrogen energy and exergy efficiencies as a function of the S/B, with (red star and square) and without H_2 spilling at S/B = 1.25.

The energy and exergy efficiencies of the whole system are shown in Figure 9. Within the S/B range 0.12–1.25, the energy efficiency shows an almost flat trend, with slight variations ranging from 0.34 to 0.36, reaching the maximum values at S/B = 0.75. The reduction in heat and electricity yields is compensated by the constant increase in hydrogen production, as shown above (see Figure 7). Since the heat is a low-grade form of energy, the corresponding exergy values are low, so the reduction in heat production has minimal effects on the total exergy output. Furthermore, hydrogen is a high-grade form of energy that increases as the S/B increases. These features are reflected in an almost linear increasing trend of exergy when steam is used as a gasification medium (S/B > 0). The maximum global exergy efficiency of the whole system is 0.33 at S/B = 1.25. The red indicators show that spilling hydrogen to cover the residual heat demand reduces the energy and exergy efficiencies by 3%.

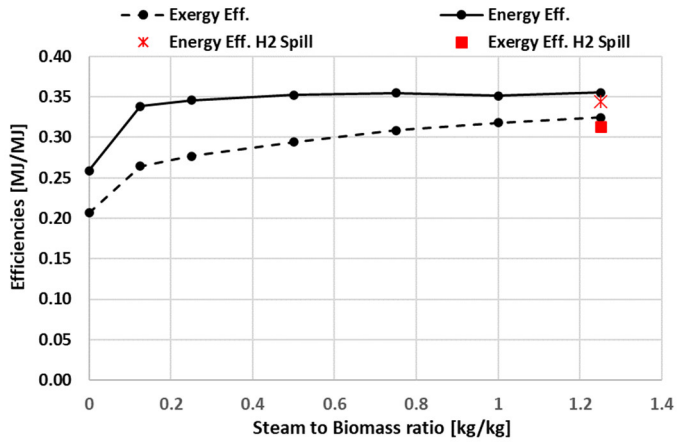

Figure 9. Global energy and exergy efficiencies as a function of the S/B, with (red star and square) and without H_2 spilling at S/B = 1.25.

Integrated Renewability (IR) has been defined in this work considering the direct consumption and substitution of non-renewable exergy resources. Figure 10 shows that the maximum IR (1.73) is obtained at S/B = 0.125. Higher steam values lead to a progressive reduction in the IR due to the progressive increase in the NG introduced to keep the off-gas at desired LHV values. Despite the use of NG, the IR is >1 except at S/B = 1.25, meaning that more non-renewable exergy is avoided by using secondary exergy streams (heat and

power) than the non-renewable exergy used in the proposed bio-hydrogen process. If bio-hydrogen is spilled to cover residual heat demand for air pre-heating and feedstock drying, the IR is still very close to the full renewability (0.99).

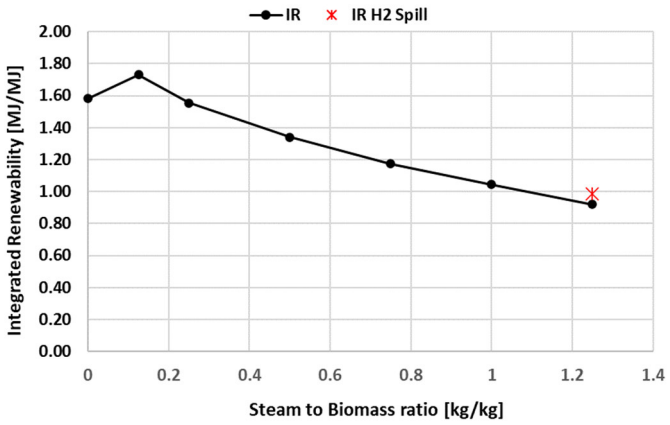

Figure 10. Integrated Renewability as function of the S/B, with (red star) and without H_2 spilling at S/B = 1.25.

The non-biogenic emissions per unit mass of bio-hydrogen production ($kg_{CO2\text{-}eq}/kg_{H2}$) are analyzed in Figure 11. With the substitution approach applied to the use of the secondary products (heat and power) in the juice production factory, the carbon dioxide emissions associated with the proposed bio-hydrogen system have negative values in the whole range of the investigated conditions. Similar to the IR, the results of the non-biogenic emissions show that the system integration avoids more non-biogenic carbon dioxide than released. The negative emissions result from applying the substitution method to the cogenerated streams (heat and power). The biogenic CO_2 emitted with the process is considered climate neutral. Figure 11 also indicates that process configuration with hydrogen spilling reduces by 47% the carbon emissions at S/B = 1.25, compared to the case when the residual heat demand is covered by additional methane consumption, leading to negative carbon emissions that equal −1.9 $kg_{CO2\text{-}eq}/kg_{H2}$. In the proposed bio-hydrogen system, the lower the S/B, the higher the contribution to mitigating the local carbon footprint.

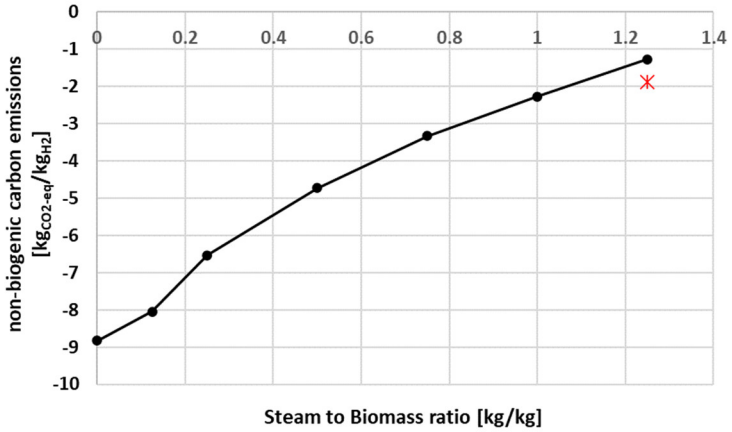

Figure 11. Non-biogenic CO_2-eq emissions as a function of the S/B, with (red star) and without H_2 spilling at S/B = 1.25.

Taking into account the annual availability of citrus peel in the region of Sicily, which is about 62,645 t on a dry basis [25] (corresponding to 348,027 t of fresh residue), it is possible to infer from Figure 7 that the regional capacity of bio-hydrogen from citrus peel is 2512 t per year. This production capacity can be used to power about 215 full-electric hybrid mini-buses (fuel cells and batteries) for public transportation (0.16 kg_{H2}/km) [26,27]. Considering a geographic area with a more expanded citrus processing industry, in Florida, it is possible to generate about 270,000 t of citrus peel on a dry basis (2018–2019) [28]. In this case, the capacity of bio-hydrogen production from citrus peel is 10,827 t per year on a state scale, while generating 480,600 GJ of net electricity.

4. Conclusions

The present work analyses an alternative polygeneration system to produce bio-hydrogen with negative carbon emissions. The proposed approach is based on residual biomass gasification with high moisture content and allows the exploitation of the PSA off-gas in a combined heat and power production process. The gasifier is operated at 850 °C and variable steam to biomass ratio (S/B) from 0 to 1.25. In this work, the off-gas composition is improved by mixing it with amounts of natural gas to increase the LHV of the off-gas to 5.4 MJ/Nm^3 (value recommended by the engine manufacturer) in every condition. Furthermore, it has been observed that the NG rate increases as the S/B in the gasifier increases.

The cogenerated (in the CHP unit) and recovered heat is mainly used to cover the internal heat demands (feedstock drying and heating the gasification mediums), while a fraction of cogenerated power is used for internal consumption. The net available heat and power are used in the juice factory. In general, the higher the steam to biomass ratio of the gasification process, the lower the net available heat that can be used in the juice factory. The following points summarize the main outcomes of the project.

(1) Highest hydrogen yield is 40 kg_{H2}/t_{db} at S/B = 1.25 and 850 °C, which is the maximum S/B investigated in this work.
(2) At the same operating conditions, 1793 MJ/t_{db} of net electricity are co-generated.
(3) The integrated renewability (IR) reached the minimum value of 0.99 at S/B = 1.25. This result indicates that the proposed bio-hydrogen production has almost-full renewability even at the worst-performing condition from the renewability viewpoint.
(4) There is −1.9 $kg_{CO2\text{-}eq}/kg_{H2}$ of non-biogenic carbon emitted when 40 kg_{H2}/t_{db} is produced at S/B = 1.25.
(5) The negative emissions observed in this work, as well as the high IR, derive from the integration of the polygeneration system with the juice factory that allows substituting the use of electricity from the national grid and heat from NG with cogenerated electricity and heat (when net heat is available). The results tell that more non-biogenic $CO_{2\text{-}eq}$ and non-renewable resources are avoided than are released and used, respectively. This work considers the direct impacts of avoided or used fossil fuels. In the case of electricity from the national grid, emission factors and non-renewable primary energy sources are obtained from datasets calculated according to the Standard IPCC methodology.
(6) Efficiency-related indicators (energy and exergy efficiencies) show the best performing conditions at the highest S/B.
(7) The integrated renewability and the non-biogenic CO_2 emissions decrease as the S/B increases. However, the carbon emissions are always negative in the investigated conditions.

The proposed systems allow the production of bio-hydrogen from wet bio-residues, such as citrus peel, with minimal use of fossil fuels and favorable impacts on the mitigation of carbon dioxide emissions by generating negative emissions due to the utilization of cogenerated energy streams (heat and power). The results presented in this

work are critical for the subsequent techno-economic studies comparing the proposed process with others available in the literature and applied to wet residual biomass. Further investigations on proper off-gas utilization and energy stream management are needed to find the best process configurations, which should come from a detailed techno-economic and techno-environmental analysis.

Author Contributions: Conceptualization, M.P.; Formal analysis, M.P. and A.P.; Funding acquisition, A.G.; Investigation, M.P. and A.G.; Methodology, M.P. and A.G.; Resources, A.P.; Software, M.P. and M.F.P.; Supervision, A.P. and A.G.; Visualization, M.F.P.; Writing—original draft, M.P.; Writing—review & editing, M.P. and A.G. All authors have read and agreed to the published version of the manuscript.

Funding: This research received no external funding.

Institutional Review Board Statement: Not applicable.

Informed Consent Statement: Not applicable.

Data Availability Statement: Not applicable.

Conflicts of Interest: The authors declare no conflict of interest.

Appendix A

Table A1 shows the main properties of the streams represented in Figure 1 of the manuscript. The values reported in the table refer to 1176 kg/h of dry biomass at 15% of moisture content (1000 kg/h on a dry basis) when the gasifier is operated at a Steam to Biomass ratio (S/B) of 1.25, temperature of 850 °C, and Equivalence Ratio (ER) of 0.3.

Table A1. Physical properties and composition of the streams represented in Figure 1 at S/B = 1.25.

	Physical Properties				Composition: Mass Fraction						
Stream Code	**Rate (t/h)**	**Temperature (K)**	**Pressure (MPa)**	**c_p (MJ/kg °C)**	**H_2O**	**N_2**	**H_2**	**CO**	CO_2	CH_4	O_2
2 (dry biom)	1.176	298	0.101	1.229							
3	3.834	1023	0.101	1.794	0.317	0.338	0.015	0.081	0.238	0.011	
4	3.834	501	0.101	1.557	0.317	0.338	0.015	0.081	0.238	0.011	
5	3.834	473	0.101	1.545	0.317	0.338	0.015	0.081	0.238	0.011	
6	3.834	473	0.101	1.545	0.317	0.338	0.015	0.081	0.238	0.011	
7	2.630	313	0.101	1.273		0.492	0.022	0.117	0.347	0.016	
8	2.630	323	0.248	1.302		0.492	0.022	0.117	0.347	0.016	
9	2.630	463	0.700	1.363		0.492	0.022	0.117	0.347	0.016	
10	2.630	380	0.700	1.333		0.492	0.022	0.117	0.347	0.016	
11	0.040	303	0.200	14.290			1.000				
12	0.040	548	1.000	14.550			1.000				
13	0.040	363	1.000	14.450			1.000				
14	0.040	323	1.000	14.370			1.000				
15	0.040	585	5.000	14.570			1.000				
16	0.040	383	5.000	14.550			1.000				
17	0.040	348	5.000	14.550			1.000				
18	0.040	674	30.000	14.680			1.000				
19	0.040	674	30.000	14.680			1.000				
20	2.590	303	0.200	1.000		0.500	0.007	0.119	0.353	0.016	
21	6.440	423	0.150	1.055	0.040	0.662			0.230		0.068
22	1.670	293	0.200	1.010		0.770					0.23
23	1.670	523	0.200	1.040		0.770					0.23
24	1.250	293	0.200	3.520	1.000						
25	1.250	298	0.200	3.540	1.000						
26	1.250	303	0.200	3.550	1.000						
27	1.250	343	0.200	3.730	1.000						
28	1.250	523	0.200	1.980	1.000						

29	0.000	353	0.210	3.770	1.000	
30	3.390	353	0.210	3.770	1.000	
31	0.000	353	0.210	3.770	1.000	
32	3.390	353	0.210	3.770	1.000	
33	1.900	353	0.210	3.770	1.000	
34	1.900	393	0.210	4.010	1.000	
35	0.000	393	0.210	4.010	1.000	
36	1.490	353	0.210	3.770	1.000	
37	29.110	353	0.210	3.770	1.000	
38	1.490	353	0.210	3.770	1.000	
39	1.490	372	0.210	3.880	1.000	
40	1.490	393	0.210	4.010	1.000	
41	0.000	393	0.210	4.010	1.000	
42	1.490	393	0.210	4.010	1.000	
43	3.390	393	0.210	4.010	1.000	
44	0.000	393	0.210	4.010	1.000	
45	3.390	393	0.210	4.010	1.000	
46	3.390	353	0.210	3.770	1.000	
47	0.058	298	0.400	2.238		1.000

References

1. IEA. *Net Zero by 2050: A Roadmap for the Global Energy Sector*; International Energy Agency: Paris, France, 2021; 224p.
2. IEA. *Global Hydrogen Review 2021*; IEA: Paris, France, 2021.
3. Prestipino, M.; Palomba, V.; Vasta, S.; Freni, A.; Galvagno, A. A Simulation Tool to Evaluate the Feasibility of a gasification-I.C.E. System to Produce Heat and Power for Industrial Applications. *Energy Procedia* **2016**, *101*, 1256–1263.
4. Basu, P. *Biomass Gasification and Pyrolysis*; Elsevier: London, UK, 2013; ISBN 9780123749888.
5. Galvagno, A.; Prestipino, M.; Maisano, S.; Urbani, F.; Chiodo, V. Integration into a citrus juice factory of air-steam gasification and CHP system: Energy sustainability assessment. *Energy Convers. Manag.* **2019**, *193*, 74–85. https://doi.org/10.1016/j.enconman.2019.04.067.
6. Prestipino, M.; Salmeri, F.; Cucinotta, F.; Galvagno, A. Thermodynamic and environmental sustainability analysis of electricity production from an integrated cogeneration system based on residual biomass: A life cycle approach. *Appl. Energy* **2021**, *295*. https://doi.org/10.1016/j.apenergy.2021.117054.
7. Cerone, N.; Zimbardi, F. Effects of oxygen and steam equivalence ratios on updraft gasification of biomass. *Energies* **2021**, *14*, 2675. https://doi.org/10.3390/en14092675.
8. Siedlecki, M.; de Jong, W.; Verkooijen, A.H.M. Fluidized bed gasification as a mature and reliable technology for the production of bio-syngas and applied in the production of liquid transportation fuels—A review. *Energies* **2011**, *4*, 389–434. https://doi.org/10.3390/en4030389.
9. Salkuyeh, Y.K.; Saville, B.A.; MacLean, H.L. Techno-economic analysis and life cycle assessment of hydrogen production from different biomass gasification processes. *Int. J. Hydrogen Energy* **2018**, *43*, 9514–9528. https://doi.org/10.1016/j.ijhydene.2018.04.024.
10. Warnecke, R. Gasification of biomass: Comparison of fixed bed and fluidized bed gasifier. *Biomass Bioenergy* **2000**, *18*, 489–497. https://doi.org/10.1016/S0961-9534(00)00009-X.
11. McKendry, P. Energy production from biomass (part 3): Gasification technologies. *Bioresour. Technol.* **2002**, *83*, 55–63. https://doi.org/10.1016/S0960-8524(01)00120-1.
12. Murthy, B.N.; Sawarkar, A.N.; Deshmukh, N.A.; Mathew, T.; Joshi, J.B. Petroleum coke gasification: A review. *Can. J. Chem. Eng.* **2014**, *92*, 441–468. https://doi.org/10.1002/cjce.21908.
13. Larson, E.D.; Jin, H.; Celik, F.E. Large-scale gasification-based coproduction of fuels and electricity from switchgrass. *Biofuels Bioprod. Biorefining* **2009**, *3*, 174–194. https://doi.org/10.1002/bbb.
14. Spath, P.; Ringer, M. Biomass to Hydrogen Production Detailed Design and Economics Utilizing the Battele Columbus Laboratory Indirectly-Heated Gasifier. NREL .2005. Available online: https://www.nrel.gov/docs/fy05osti/37408.pdf (accessed on 25 June 2022).
15. Pallozzi, V.; Di Carlo, A.; Bocci, E.; Villarini, M.; Foscolo, P.U.; Carlini, M. Performance evaluation at different process parameters of an innovative prototype of biomass gasification system aimed to hydrogen production. *Energy Convers. Manag.* **2016**, *130*, 34–43. https://doi.org/10.1016/j.enconman.2016.10.039.
16. Yao, J.; Kraussler, M.; Benedikt, F.; Hofbauer, H. Techno-economic assessment of hydrogen production based on dual fluidized bed biomass steam gasification, biogas steam reforming, and alkaline water electrolysis processes. *Energy Convers. Manag.* **2017**, *145*, 278–292. https://doi.org/10.1016/j.enconman.2017.04.084.
17. Binder, M.; Kraussler, M.; Kuba, M.; Luisser, M. *Hydrogen from Biomass Gasification—IEA Bioenergy*; Paris, France, 2018; Volume Task 33.

18. Cerone, N.; Zimbardi, F.; Villone, A.; Strjiugas, N.; Kiyikci, E.G. Gasification of Wood and Torrefied Wood with Air, Oxygen, and Steam in a Fixed-Bed Pilot Plant. *Energy Fuels* **2016**, *30*, 4034–4043. https://doi.org/10.1021/acs.energyfuels.6b00126.
19. You, S.; Tong, H.; Armin-Hoiland, J.; Tong, Y.W.; Wang, C.H. Techno-economic and greenhouse gas savings assessment of decentralized biomass gasification for electrifying the rural areas of Indonesia. *Appl. Energy* **2017**, *208*, 495–510. https://doi.org/10.1016/j.apenergy.2017.10.001.
20. Ptasinski, K.J. *Efficiency of Biomass Energy*; John Wiley & Sons: Hoboken, NJ, USA, 2015; ISBN 9781118702109.
21. ISPRA Fattori di Emissione per la Produzione ed il Consumo di Energia Elettrica in Italia. Available online: http://www.sinanet.isprambiente.it/it/sia-ispra/serie-storiche-emissioni/fattori-di-emissione-per-la-produzione-ed-il-consumo-di-energia-elettrica-in-italia/view (accessed on 25 June 2022).
22. Jarungthammachote, S.; Dutta, A. Equilibrium modeling of gasification: Gibbs free energy minimization approach and its application to spouted bed and spout-fluid bed gasifiers. *Energy Convers. Manag.* **2008**, *49*, 1345–1356. https://doi.org/10.1016/j.enconman.2008.01.006.
23. Cormos, A.M.; Dragan, S.; Cormos, C.C. Integration of membrane technology for decarbonization of gasification power plants: A techno-economic and environmental investigation. *Appl. Therm. Eng.* **2022**, *205*, 118078. https://doi.org/10.1016/j.applthermaleng.2022.118078.
24. Prestipino, M.; Chiodo, V.; Maisano, S.; Zafarana, G.; Urbani, F.; Galvagno, A. Hydrogen rich syngas production by air-steam gasification of citrus peel residues from citrus juice manufacturing: Experimental and simulation activities. *Int. J. Hydrogen Energy* **2017**, *42*, 26816–26827. https://doi.org/10.1016/j.ijhydene.2017.05.173.
25. Famoso, F.; Prestipino, M.; Brusca, S.; Galvagno, A. Designing sustainable bioenergy from residual biomass: Site allocation criteria and energy/exergy performance indicators. *Appl. Energy* **2020**, *274*, 115315. https://doi.org/10.1016/j.apenergy.2020.115315.
26. Napoli, G.; Micari, S.; Dispenza, G.; Di Novo, S.; Antonucci, V.; Andaloro, L. Development of a fuel cell hybrid electric powertrain: A real case study on a Minibus application. *Int. J. Hydrogen Energy* **2017**, *42*, 28034–28047. https://doi.org/10.1016/j.ijhydene.2017.07.239.
27. Dispenza, G.; Sergi, F.; Napoli, G.; Randazzo, N.; Di Novo, S.; Micari, S.; Antonucci, V.; Andaloro, L. Development of a solar powered hydrogen fueling station in smart cities applications. *Int. J. Hydrogen Energy* **2017**, *42*, 27884–27893. https://doi.org/10.1016/j.ijhydene.2017.07.047.
28. Fried, N.; Hudson, M.E. Florida Citrus Statistics 2018–2019. 2020. Available online: https://www.nass.usda.gov/Statistics_by_State/Florida/Publications/Citrus/Citrus_Statistics/index.php (access on 25 June 2022). .